

Experimental evaluation of a two-photon wave packet in type-II parametric downconversion

A. V. Sergienko, Y. H. Shih, and M. H. Rubin

Department of Physics, University of Maryland Baltimore County, Baltimore, Maryland 21228

Received April 5, 1994; revised manuscript received October 18, 1994

A two-photon wave packet (a biphoton) produced by type-II parametric downconversion is studied in a simple beam-splitting experiment for its natural shape in space-time. The measured triangular shape of a two-photon correlation function is the signature of a rectangular-shaped biphoton. Inserting a birefringent sample into the beam causes a displacement of the vertex of the notch pattern, which can be used to measure the optical delay between the ordinary and the extraordinary rays in the sample with femtosecond resolution.

Two-particle entangled states have been known since the early days of quantum mechanics. Entangled states are states of two or more particles that cannot be written as products of single-particle states. These states play an important role in the study of the Einstein-Podolsky-Rosen paradox¹ and in the test of Bell's inequalities.²

In spontaneous parametric downconversion (SPDC) a pump beam is incident upon a birefringent crystal. The pump beam is intense enough that nonlinear effects lead to the spontaneous emission of a pair of entangled light quanta by means of the well-known phase-matching condition^{3,4}

$$\omega_1 + \omega_2 = \omega_p, \quad \mathbf{k}_1 + \mathbf{k}_2 = \mathbf{k}_p, \quad (1)$$

where ω_i is the frequency and \mathbf{k}_i is the wave vector, linking pump (p), signal (1), and idler (2). The downconversion is called Type I or Type II, depending on whether the photons in the pair have parallel or orthogonal polarizations. The light quanta of the pair that emerges from the nonlinear crystal may propagate in different directions or may propagate collinearly. The frequency and propagation directions are determined by the orientation of the nonlinear crystal and the phase-matching relations in Eqs. (1). Type-I SPDC was used intensively as a convenient source of two-photon entangled states.⁵⁻⁹

It was shown recently^{10,11} that Type-II SPDC provides much richer physics owing to the two-photon entanglement both in space-time and in spin. It is even possible to demonstrate violations of Bell's inequalities for both space-time and spin variables in a single experimental setup.¹² The two-photon dispersion of the ordinary and the extraordinary waves in a nonlinear crystal lead to a space-time structure of a wave function that is completely different from that generated in a Type-I SPDC. We have developed a new approach to the measurement of the natural shape and width of a two-photon wave function. This technique also allows us to measure with femtosecond resolution time delays in optical materials that are due to the difference in group velocities of the two polarizations. It provides better time resolution, stability, and statistical accuracy than techniques based on Type-I SPDC interferometers.¹³⁻¹⁵

For collinear Type-II SPDC the two-photon part of the

state that emerges from the downconversion crystal may be calculated from the standard theory of SPDC (first-order perturbation theory) to be^{3,4}

$$|\Psi\rangle = \int d\omega_1 \delta(\omega_1 + \omega_2 - \omega_p) \psi(k_1 + k_2 - k_p) a_o^\dagger[\omega_1(k_1)] \times a_e^\dagger[\omega_2(k_2)] |0\rangle, \quad (2)$$

where ω and k represent the frequency and the wave number, respectively, for signal (1), idler (2), and pump (p). The subscripts o and e on the creation operators indicate the ordinary and the extraordinary rays of the downconversion, traveling along the same direction as the pump, the z direction. The coordinate axes x and y are chosen along the polarization direction of the o ray and the e ray, respectively. The use of small apertures makes the state in Eq. (2) a good one-dimensional approximation. The frequency phase-matching condition is explicitly displayed by the delta function; the wave-number phase-matching condition is not of the form $\delta(k_1 + k_2 - k_p)$ because of the finite length of the crystal.^{3,4} The function Ψ determines the natural spectral width of the two-photon state. Taking the origin of the coordinates at the output surface of the downconversion crystal, we obtain

$$\psi(\Delta k) = [1 - \exp(-i\Delta k L)]/(i\Delta k L), \quad (3)$$

where L is the length of the crystal and $\Delta k = k_1 + k_2 - k_p$.

Suppose that the crystal is oriented so that the perfect phase-matching condition, Eq. (1), is satisfied by a set Ω_o , Ω_e , k_o , and k_e (in this experiment we choose $\Omega_o = \Omega_e$). Because of the finite bandwidth of the two-photon state we may let $\omega_1 = \Omega_o + \nu$ and $\omega_2 = \Omega_e - \nu$, where $|\nu| \ll \Omega_{o,e}$. Now expand k_1 and k_2 to the first order in ν using the dispersion relations

$$k_1 = k_o + \nu(dk_o/d\Omega_o) = k_o + \nu/u_o, \\ k_2 = k_e - \nu(dk_e/d\Omega_e) = k_e - \nu/u_e,$$

where u_o (u_e) is the group velocity for the ordinary (extraordinary) ray. Equation (3) can be written as

$$\psi(\nu) = [1 - \exp(-i\nu DL)]/i\nu D, \quad (4)$$

where $D = 1/u_o - 1/u_e$. We assume a negative crystal (β -BaB₂O₆, BBO), i.e., $u_e > u_o$.

Consider the experimental setup of Fig. 1. First suppose that no quartz plates are placed between the BBO crystal and the beam splitter. The fields at detectors 1 and 2 are given by

$$E_1^{(+)}(t) = \alpha_t \int d\omega \exp[-i\omega(t - \tau_1)] \sum_j \hat{e}_1 \cdot \hat{e}_j a_j(\omega),$$

$$E_2^{(+)}(t) = \alpha_r \int d\omega \exp[-i\omega(t - \tau_2)] \sum_j \hat{e}_2 \cdot \hat{e}_j a_j(\omega), \quad (5)$$

where a_j is the annihilation operation of the photons, $j = o, e$, \hat{e}_i is in the direction of the i th linear polarization analyzer axis, $i = 1, 2$, and $\tau_i = s_i/c$, where s_i is the optical path length from the output surface of the BBO crystal to the i th detector, and c is the speed of light. We assume that $\tau_1 = \tau_2$ for the following discussion. α_t and α_r are the complex transmission and reflection coefficients of the 50:50 beam splitter. The average coincidence counting rate is given by

$$R_c = (1/T) \iint_0^T dT_1 dT_2 |\Psi(t_1, t_2)|^2, \quad (6)$$

where $t_i \equiv T_i - \tau_i$ and T_i is the detection time of the i th detector. T is the duration time of the measurement. An effective two-photon wave function $\Psi(t_1, t_2)$ is defined in Eq. (6),

$$\Psi(t_1, t_2) = \langle 0 | E_1^{(+)} E_2^{(+)} | \Psi \rangle. \quad (7)$$

Substituting Eqs. (2) and (5) into Eq. (7) and taking the analyzer angle to be 45° give

$$\Psi(t_1, t_2) = \alpha_t \alpha_r v(t_1 + t_2) [u(t_1 - t_2) - u(-t_1 + t_2)], \quad (8)$$

where

$$v(t) = v_0 \exp(-i\omega_p t/2), \quad (9)$$

$$u(t) = u_0 \exp(-i\omega_d t/2) \int_{-\infty}^{\infty} d\nu [1 - \exp(-\nu DL)] / (i\nu DL) \\ \times \exp(-i\nu t) \\ = \exp(-i\omega_d t/2) \Pi(t). \quad (10)$$

Here $\Pi(t)$ is

$$\Pi(t) = \begin{cases} u_0 & DL > t > 0, \\ 0 & \text{otherwise} \end{cases}, \quad (11)$$

where v_0 and u_0 are constants (normalization) and $\omega_d = \Omega_o - \Omega_e$. We have approximated the pump to be a plane wave (single mode) in the calculation. If the pump beam were taken to be a Gaussian with bandwidth σ_p , the constant v_0 would be replaced by a Gaussian function $v_0 \exp(-\sigma_p^2 t^2/8)$. In this case we may write the effective wave function in the following form:

$$\Psi(t_1, t_2) = v_0 \exp(-\sigma^2(t_1 + t_2)^2/8) \Pi(t_1 - t_2) \exp(-i\Omega_o t_1) \\ \times \exp(-i\Omega_o t_2). \quad (12)$$

A schematic of the $\Pi(t)$ part of a two-photon wave function is shown in Fig. 2.

It is not difficult to understand the physics of the effective two-photon wave function, Eq. (8). In the first term in the brackets the o ray goes to detector 1 and the e ray goes to detector 2; the rectangular-shaped function $u(t_1 - t_2)$ implies that if detector 2 is triggered at T_2 then detector 1 will be triggered at a later time, $T_2 < T_1 < T_2 + DL$. In the second term the e ray goes to detector 1 and the o ray goes to detector 2; the rectangular function $u(-t_1 + t_2)$ implies that if detector 1 is triggered at T_1 then detector 2 will be triggered at a later time, $T_1 < T_2 < T_1 + DL$. The joint triggering probability at T_1 and T_2 is a constant during these periods and is zero otherwise. The two-dimensional wave packet (biphoton) has an infinite width along the axis of $t_1 + t_2$ because the pair can be produced at any time. Along the $t_1 - t_2$ axis the width is finite. The wave packet in the first term of in brackets in Eq. (8) is centered at $DL/2$, and the wave packet in the second term is centered at $-DL/2$. This represents a reasonable physical picture for Type-II SPDC, because each photon pair contains an o ray and an e ray. BBO is a negative uniaxial crystal, so the e ray emerges from the BBO crystal first. The maximum possible time

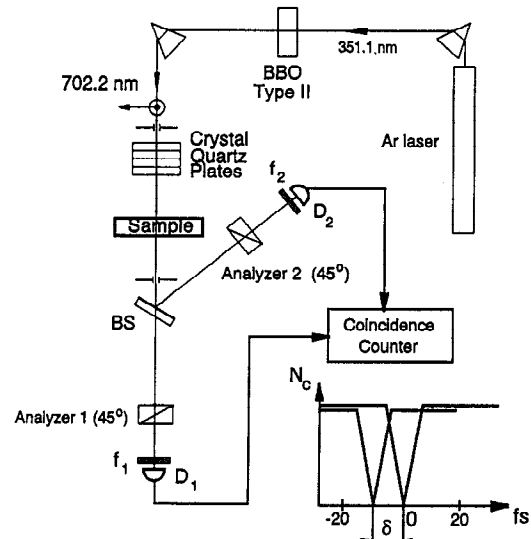


Fig. 1. Schematic of the experimental setup. BS, beam splitter; f_1, f_2 , spectral filters; D_1, D_2 , single-photon detector packages; N_c , coincidence count.

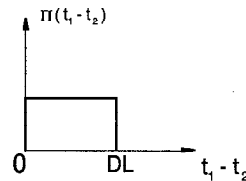


Fig. 2. Schematic of the $\Pi(t)$ part of a two-photon wave function.

delay between the *o* ray and *e* ray is $(L/u_o - L/u_e) = DL$, which is the time delay for crossing the entire crystal.

It is interesting to see that the two terms in the effective wave function, Eq. (8), do not show any interference because they do not overlap in space-time. Physically this means that is impossible to find any detection time T_1 or T_2 for which the two terms in Eq. (8) are both nonzero (except for the negligible case when $T_1 = T_2$).

Now consider the case in which an additional birefringent material is placed between the BBO and the beam splitter. We place a piece of birefringent material (crystal quartz, for instance) in such a way that the fast axis of the material coincides with the slow axis of the BBO, as shown in Fig. 1. In this case the effective wave function becomes (again the analyzers are set at 45°)

$$\Psi(T_1, T_2) = \alpha_t \alpha_v [u(T_1 - T_2 + \delta) - u(-T_1 + T_2 + \delta)], \quad (13)$$

where $\delta = (l_e - l_o)/c$ is the optical delay in the crystal quartz and ϕ is a phase constant that is related to the sum of l_e and l_o . It is easy to see from Eq. (13) that the two terms in the bracket can now overlap. When $\delta = DL/2$, they are completely overlapped and cancel each other.

The measured coincidence counting rate R_c is calculated by substitution of Eq. (13) into Eq. (6),

$$R_c = R_{c0}[1 - \rho(\delta)], \quad (14)$$

where ρ is a Λ -shaped function of δ (self-convolution of the rectangular wave function),

$$\rho = \begin{cases} 0 & -\infty < \delta < 0 \\ \kappa\delta & 0 < \delta \leq DL/2 \\ 1 - \kappa(\delta - DL/2) & DL/2 \leq \delta < DL \\ 0 & DL < \delta < \infty \end{cases}, \quad (15)$$

and $\kappa = 2/DL$, resulting in a V-shaped R_c . It is easy to see that the width and the shape of the biphoton can be evaluated by the width and the shape of R_c .

If a sample of optical material is placed in the optical path, the time delay δ between the *o* ray and the *e* ray in the sample can be estimated by measurement of the displacement of the vertex of the V-shaped function, as is shown in Fig. 3. It is not difficult to achieve a subfemtosecond accuracy by use of a shorter crystal (smaller DL).

The schematic experimental setup is illustrated in Fig. 1. A cw argon-ion laser line of 351.1 nm was used to pump an 8 mm \times 8 mm \times (0.56 \pm 0.05) mm BBO nonlinear crystal. The BBO was cut at a Type-II phase-matching angle, $\Theta = 48^\circ$ relative to the optic axis to generate a pair of directionally collinear orthogonally polarized signal and idler photons at a 702.2-nm wavelength. The downconverted beams were directed at a near-normal incidence angle to a polarization-independent beam splitter, which has 50%–50% reflection and transmission coefficients. A single-photon detector package is placed in each transmission and reflection output port of the beam splitter. Each package includes a 24.5-mm-diameter convex lens to focus radiation down onto the photosensitive area of the detector, which is 0.8 mm in diameter. The photon detectors are dry-ice-cooled avalanche photodiodes operated in a

photon-counting Geiger mode. A Glan-Thompson linear polarization analyzer, followed by a spectral filter with 83 nm FWHM bandwidth, which is used mainly to cut off the UV scattered radiation from the pump, is placed in front of each of the detectors packages. The polarization analyzers are oriented at 45° relative to the *o* ray and the *e* ray polarization planes of the BBO crystal. The output pulses of the detectors are then sent to a coincidence circuit with a 3-ns coincidence time window.

A set of crystal quartz plates is placed between the downconversion crystal and the beam splitter for changing the optical delay δ between the signal and the idler photons. The fast axes of the quartz plates were carefully aligned to match the *o*-ray or *e*-ray polarization planes of the BBO crystal during the measurements. Each of the quartz plates is (1 \pm 0.1) mm in thickness, resulting in an optical delay of $\delta \approx 30$ fs between the *o* ray and the *e* ray at wavelengths near 700 nm. The quartz plates were aligned carefully one by one before data were taken, and the plates were moved away one by one during the measurements.

Figure 3 shows the observed V-shaped coincidence-rate measurements as a function of the optical delay δ . The coincidence counts are direct measurements with no accidental-coincidence subtractions or any other theoretical corrections. The V-shaped curves are the fits for Eq. (15). Each of the data points corresponds to different numbers of quartz plates remaining in the path of the signal and the idler beams. The data indicated by the dashed curve were obtained when an additional 2.4-mm-thick test sample of crystal quartz was introduced into the beam right in front of the beam splitter. Comparing the results indicated by the solid and the dashed curves, we find that the vertex has a displacement of $\delta = (72 \pm 3)$ fs, which corresponds to the propagation time delay of ordinary and extraordinary waves in a 2.4-mm quartz sample. Our quartz sample was specially selected to compensate for the optical delay between the ordinary and the extraordinary waves inside the nonlinear crystal. We have found from the literature data for the group-velocity dispersion of ordinary and extraordinary waves in BBO crystal that $D = (1/u_o - 1/u_e) \approx 2.5$ ps/cm in the degenerate case of $\lambda_1 = \lambda_2 = 702.2$ nm. Therefore, on the basis of the thickness of our crystal, we can estimate the

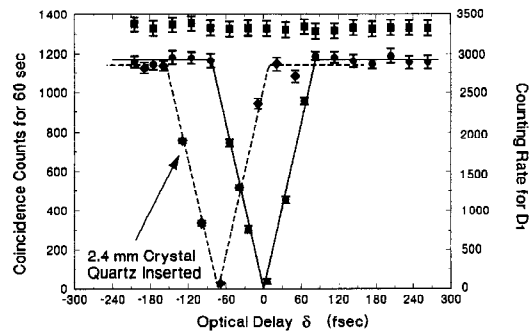


Fig. 3. Observation of a V-shaped correlation function and measurement of optical delay in a 2.4-mm-thick sample of crystal quartz.

size of the half-base of the triangle, $DL/2 = (70 \pm 6)$ fs. The measured value of δ coincides with our prediction within experimental error. Uncertainty in the crystal thickness measurement is the main contribution to the error of this comparison.

In conclusion, the natural rectangular shape of the space-time structure of the two-photon effective wave function (biphoton) in Type-II parametric downconversion was verified by the observation of a V-shaped correlation function. The optical delay between orthogonally polarized waves in the sample of birefringent material was measured with a 3-fs resolution. This approach can be used to measure optical delays or related parameters in fibers, nonlinear crystals, or optically active media and to study group-velocity dispersions in different optical processes. Subfemtosecond resolution can be achieved by the use of a shorter nonlinear crystal.

ACKNOWLEDGMENTS

We thank D. N. Klyshko for helpful discussions. This research is supported by U.S. Office of Naval Research grant N00014-91-J-1430.

REFERENCES

1. A. Einstein, B. Podolsky, and N. Rosen, *Phys. Rev.* **47**, 777 (1935).
2. J. S. Bell, *Physics* **1**, 195 (1964).
3. D. N. Klyshko, *Photons and Nonlinear Optics* (Gordon & Breach, New York, 1988).
4. A. Yariv, *Quantum Electronics* (Wiley, New York, 1967).
5. Y. H. Shih and C. O. Alley, *Phys. Rev. Lett.* **61**, 2921 (1988).
6. Z. Y. Ou and L. Mandel, *Phys. Rev. Lett.* **61**, 50 (1988).
7. C. K. Hong, Z. Y. Ou, and L. Mandel, *Phys. Rev. Lett.* **59**, 2044 (1987).
8. Z. Y. Ou and L. Mandel, *Phys. Rev. Lett.* **61**, 54 (1988); P. G. Kwiat, A. M. Steinberg, and R. Y. Chiao, *Phys. Rev. A* **47**, 2472 (1993).
9. J. Brendel, E. Mohler, and W. Martienssen, *Phys. Rev. Lett.* **66**, 1142 (1991); T. S. Larchuk, R. A. Campos, J. G. Rarity, P. R. Tapster, E. Jakeman, B. E. A. Saleh, and M. C. Teich, *Phys. Rev. Lett.* **70**, 1603 (1993).
10. T. E. Kiess, Y. H. Shih, A. V. Sergienko, and C. O. Alley, *Phys. Rev. Lett.* **71**, 3893 (1993).
11. Y. H. Shih and A. V. Sergienko, *Phys. Lett. A* **186**, 29 (1994).
12. Y. H. Shih and A. V. Sergienko, *Phys. Rev. A* **50**, 2564 (1994).
13. A. M. Steinberg, P. G. Kwiat, and R. Y. Chiao, *Phys. Rev. Lett.* **71**, 708 (1993).
14. C. K. Hong, Z. Y. Ou, and L. Mandel, *Phys. Rev. Lett.* **59**, 1903 (1987).
15. J. G. Rarity and P. R. Tapster, *J. Opt. Soc. Am. B* **6**, 1221 (1989).